Check for updates

Water Science & Technology

IWA PUBLISHING

© 2022 The Authors

Water Science & Technology Vol 86 No 5, 1122 doi: 10.2166/wst.2022.255

Electrochemical oxidation process on palm oil mill effluent waste activated sludge: optimization by response surface methodology

Branda Jian Tong Yap[a], Gan Chin Heng[b,*] and Choon Aun Ng[a]

[a] Department of Environmental Engineering, Faculty of Engineering and Green Technology, Universiti Tunku Abdul Rahman, Jalan Universiti, Bandar Barat, Kampar 31900, Perak, Malaysia
[b] Department of Civil Engineering, Lee Kong Chian Faculty of Engineering and Science, Universiti Tunku Abdul Rahman, Jalan Sungai Long, Bandar Sungai Long, Cheras, Kajang 43000, Selangor, Malaysia
*Corresponding author. E-mail: ganch@utar.edu.my

GCH, 0000-0003-1007-3353

ABSTRACT

Biological-based treatment as the conventional treatment for palm oil mill effluent (POME) in open-ponding system face a well known rate-limiting step which is hydrolysis. In this study, electrochemical oxidation (EO) by a ruthenium oxide-coated titanium (Ti/RuO_2) electrode was introduced as a pre-treatment for POME waste activated sludge (WAS). Surface morphology and elemental analysis were investigated using field emission scanning electron microscopy and energy dispersive X-ray spectroscopy, respectively. Response surface methodology type central composite design was used in this study to understand the relationship between the independent and dependent variables. Analysis of variance (ANOVA) was used to validate the model of the studied variables. The correlation coefficients (R^2) indicated a close agreement between the experimental results and the predicted values, with high R^2 values of 0.9044–0.9773. Multiple response optimization suggested that the range of current density (17–27 mA/cm^2) and electrolysis time (55–75 min) at a fixed concentration of sodium chloride (10 g/L), resulted in mixed liquor volatile suspended solids (MLVSS) removal >20%, capillary suction timer (CST) reduction >43%, extracellular polymeric substances (EPS) increment <19% and soluble chemical oxygen demand (sCOD) increment >25%. EO appears to be an efficient pre-treatment as well as practical way to improve the POME WAS disintegration and dewaterability.

Key words: electrochemical oxidation, palm oil mill effluent, response surface methodology, Ti/RuO_2 electrodes, waste activated sludge

HIGHLIGHTS

- Electrochemical oxidation (EO) for waste activated sludge (WAS) from palm oil mill effluent (POME) was investigated.
- Current density and electrolysis time showed significant interactive effects.
- Optimum operating conditions based on CCD-RSM were ranges at current density 17–27 mA/cm^2 and electrolysis time 55–75 min, at a fixed 10 g/L of NaCl.
- Suitability of EO using Ti/RuO_2 prior to anaerobic digestion was confirmed.

This is an Open Access article distributed under the terms of the Creative Commons Attribution Licence (CC BY 4.0), which permits copying, adaptation and redistribution, provided the original work is properly cited (http://creativecommons.org/licenses/by/4.0/).

Downloaded from http://iwaponline.com/wst/article-pdf/86/5/1122/1109750/wst086051122.pdf
by guest

GRAPHICAL ABSTRACT

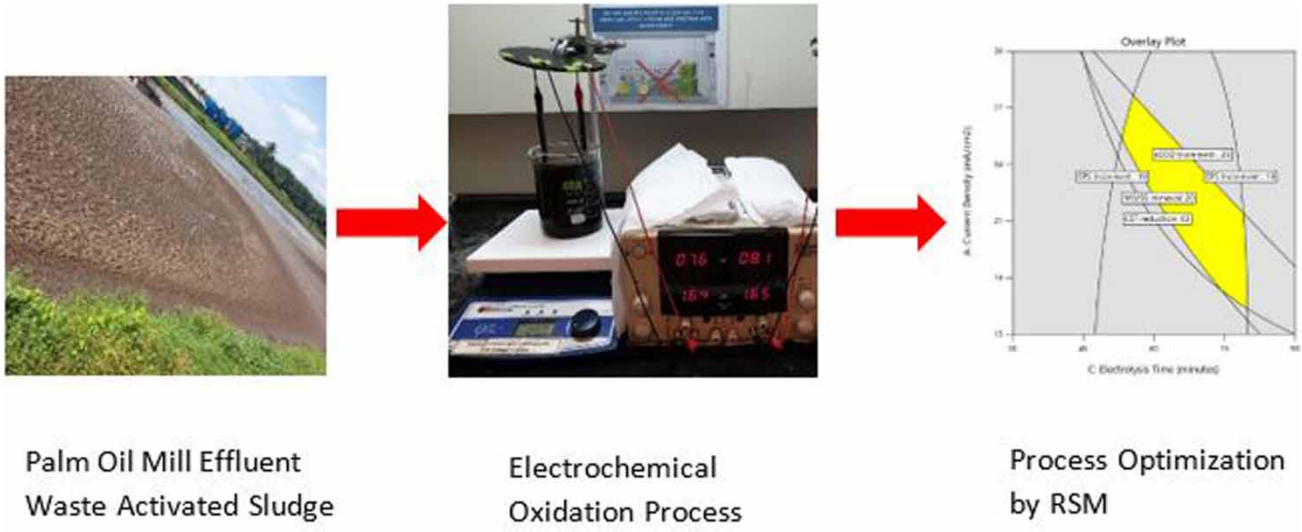

1. INTRODUCTION

The palm oil industry has always been a very popular and crucial contributor to the economy of Malaysia. Over the years, the number of palm oil mills has increased gradually, consequently generating more and more by-products and waste from the palm oil mill effluent (POME). By-products have had significant impacts upon the environment as they generate excessive biological oxygen demand (BOD) and chemical oxygen demand (COD). Furthermore, POME contains excessive concentrations of organic nitrogen, phosphorus and different supplement substances. These have caused the need for treatment for POME to ensure that it stays within the threshold limit value (TLV) based on the standards set by the local environmental organisations, for instance Department of Environment (DOE), Malaysia before discharge into water bodies (Kamyab *et al.* 2018).

Biological treatment is the most common treatment technology being practiced to treat POME. However, waste activated sludge (WAS), an unwanted residue that contains high organic and solid contents with poor dewaterability will be generated after the biological treatment. Landfilling and incineration are both common ways to handle WAS, however these methods have their downside by either jeopardizing the environment or threating the living population. Anaerobic digestion (AD) has always been the conventional method for treating the sewage treatment plant (STP) WAS, whereby it could reduce its volume, to ensure that it is safe to be treated as bio-solids. In addition, AD has the capability to release biogas that can be used as a source of renewable energy. Nevertheless, due to the presence of hard-to-manage substances within the POME WAS, AD could only do so much for instance, the elimination of the biodegradable part (Nurhayati *et al.* 2020). Hydrolysis in AD has always been a drawback that limits the treatment's efficiency due to the presence of extracellular polymeric substances (EPS) like lipids, polysaccharides, fatty acids and nuclei acids that have high water binding ability. For that reason, pre-treatment is required to achieve a better performance on the overall treatment system for POME WAS.

Mechanical, thermal, chemical or biological treatments are a few common types of pre-treatment that serve the same purpose, which is to increase the solubility or reduce the size of organic compounds, so that the sludge can be degraded easily and further improve its dewatering properties (Heng *et al.* 2021). Among the pre-treatment methods, the advance oxidation process (AOP) is easily implemented and considered as a comprehensive technology in terms of its competence on degrading contaminants and its ability to conquer the shortcoming of conventional methods (Iskurt *et al.* 2021; Jiang *et al.* 2021). AOP is able to synergize with the AD process through the generation of radicals (•OH) by disrupting and destroying the cell walls that lead to the process of sludge cell disintegration (Pérez-Rodríguez *et al.* 2019). It helps in converting high molecular weight organic matter into low molecular weight matter, which then reduces the biodegradation difficulty and hence bypasses the rate-limiting step. Electrochemical oxidation (EO) is termed a clean and efficient AOP, as it has the ability to remove recalcitrant and persistent pollutants from wastewater and convert them into simpler forms (Nurhayati *et al.* 2020). The outcome of EO proves that it could be an environmentally friendly and efficient pre-treatment system for POME WAS. EO involves the

Downloaded from http://iwaponline.com/wst/article-pdf/86/5/1122/1109750/wst086051122.pdf
by guest

utilization of energy input and electrolyte to interact with contaminants in order to degrade them successfully. The mechanisms of EO start with oxidation of water molecules to form •OH radicals and induce a reaction with metal oxides that generates a high oxidizing power electrode. Following that, redox reactions of RuO_3/RuO_2 oxidize the pollutants (P); decomposition of the oxidized electrode by the oxygen evolution by-reaction is shown in the following equations (Equations (1)–(4)) (Heng *et al.* 2021):

$$RuO_2 + H_2O \rightarrow RuO_2(\bullet OH) + H^+ + e^- \quad (1)$$

$$RuO_2(\bullet OH) \rightarrow RuO_3 + H^+ + e^- \quad (2)$$

$$RuO_3 + P \rightarrow RuO_2 + PO \quad (3)$$

$$2RuO_3 \rightarrow 2RuO_2 + O_2 \quad (4)$$

The nature of the electrodes used plays a crucial role as it could influence the performance of the EO. Bare metal as electrodes is treatable but corrosion could occur. These problems were able to be resolved by introducing a coating of transition metal oxides (TMO) and mixed metal oxides (MMO) (Ken & Sinha 2021). MMO helps to reduce the percentage of corrosion current through the coating which then increases the shelf life of the electrodes. MMO coated on metal plates are also termed as dimensionally stable anodes (DSA), they are known to have an extensive service life over a vast range of current density (Johnson & Kumar 2020). Lead dioxide (PbO_2) is able to excel in the treatment, but due to its lead dissolution properties it endangers the treatment system. Tin(IV) oxide (SnO_2) possesses a shorter life span when compared with others and iridium (IV) oxide (IrO_2) lacks O_2 over-potential that causes it to be less efficient. As for ruthenium (IV) oxide (RuO_2), it has been listed as one of the most versatile and finest oxidation catalyst due to its high stability and ohmic conductivity (Ajab *et al.* 2020). For excellent chlorine evolution properties (~2.0 V), mechanical and chemical resistance in high pH conditions is needed (Johnson & Kumar 2020). Comparing MMO, RuO_2 showed a promising performance. It covers a vast range of treatments for wastewater from pharmaceutical to oil mill and even dye removal with the assistance of chlorine generated during the treatment process (Jiang *et al.* 2021). With its stability, it tends to have a longer life span when compared with other DSA. Pechini's method is an effective process used in the fabrication of DSA as the chelated metal cation and glycol undergoes polyesterification, forming covalent and coordinative bonds (Kang *et al.* 2020).

The aim of this study was to identify the optimum operating conditions for EO leading to a pre-treated sludge that is well disintegrated and dewatered for the subsequent AD treatment. The efficiencies of the pre-treatment were tested based on four dependent variables i.e., mixed liquor volatile suspended solids (MLVSS) removal, capillary suction timer (CST) reduction, EPS increment and soluble COD (sCOD) and increment on three independent variables which were current density, electrolyte concentration and electrolysis time. Current density is known to be one of the most important operating variable in EO, as higher current density would allow more electrons to pass by generating more oxidizing species (•OH radicals) to biodegrade the organic pollutants (Moteshaker *et al.* 2020). One study showed that EO promoted no biodegradability in terms of sCOD at 30–40 mA/cm^2 (Pasalari *et al.* 2021). Electrolysis time determines the reaction rate and removal efficiency of the pre-treatment (Heidari *et al.* 2020). Stagnant sCOD solubilization would gradually start to occur at 90 minutes due to the accumulation of soluble organic matter, which builds up the resistance of the system thus reducing the current (Ye *et al.* 2016). Lastly, the type of electrolyte and its concentration affect the conductivity of the EO process. For instance, sodium chloride (NaCl) at the range of 1.8–20 g/L, is able to generate oxidant species that have the quality of showing a higher reaction rate with organic compounds (Fajardo *et al.* 2017). The chloride ions from NaCl would minimize the side effects of anions such as bicarbonate (HCO_3^-) and sulfate (SO_4^{2-}), which would cause resistance to the overall treatment efficiencies. Electrolyte concentration should be limited, as excessive active chlorine species would lead to the annihilation of organic matter (Zhu *et al.* 2019). The conventional methods of determining the relationship between dependent and independent variable are rather sophisticated and time consuming. Hence, the response surface methodology (RSM), a statistical and mathematical method, was implemented due to its reliability and accuracy. RSM is popular in experiment design, model buildings, the relationship of variables evaluation and condition optimization. The most well-known technique in RSM is central composite design (CCD) for identifying the optimum operating conditions for pre-treatment by making traits need fewer experiment runs (Darvishmotevalli *et al.* 2019).

Downloaded from http://iwaponline.com/wst/article-pdf/86/5/1122/1109750/wst086051122.pdf
by guest

2. EXPERIMENTAL

2.1. Materials

The POME WAS were collected from the local palm oil mill located at Ayer Kuning, Perak, Malaysia. The collected WAS were thickened and refrigerated at 4 °C prior to any analysis and pre-treatment. The characteristics of raw POME WAS are listed in Table 1. Different stages of the experiments required different types of chemicals, together with its purposes, which are concluded in Table 2 below. The electrodes used were titanium plates with the dimensions of 150 mm × 30 mm and a thickness of 2 mm.

2.2. Synthesizing of dimensionally stable anodes (DSA)

Pechini's method was chosen for the fabrication of titanium (Ti) electrodes coated with ruthenium oxide (RuO_2). RuO_2 was chosen due to its distinction of chlorine evolution over-potential and weakening of oxygen evolution, therefore generating free radicals for organic compound oxidation (Johnson & Kumar 2020). Three stages are involved in the fabrication process. Firstly, pre-treatment of electrodes using sandpaper and isopropyl alcohol for washing purposes then boiling with 20% chloride acid and 10% oxalic acid in order to remove the titanium's oxide hydroxide coating and improve its roughness at the same time. The second stage is the preparation of precursor solution, which was EG:CA:$RuCl_3$ with the molar ratio of 10:3:1. The final stage is the coating process, 20 layers of coating was done and completed with the final calcination at 400–500 °C for 1 hour. The morphology of the coated electrodes was analyzed using field emission scanning electron microscopy (FESEM) and energy dispersive X-ray (EDX) spectroscopy.

Table 1 | Characteristics of raw palm oil mill effluent (POME) waste activated sludge (WAS)

Characteristic	Unit	Mean value
pH	–	7.92
Total Solids	mg/L	100,240
Total Volatile Solids	mg/L	84,990
Mixed Liquor Suspended Solids	mg/L	43,000
Mixed Liquor Volatile Suspended Solids	mg/L	29,800
Soluble Chemical Oxygen Demand	mg/L	855.9
Extracellular Polymeric Substances	mg/L	580.79
Capillary Suction Time	s	95.2

Table 2 | Materials and theirs purpose for EO pre-treatment

Material	Purpose
Palm Oil Mill Effluent (POME) Waste Activated Sludge (WAS)	Subject to be treated
Isopropyl Alcohol (C_3H_8O)	Synthesizing of dimensionally stable anodes (DSA)
20% of Chloride Acid ($HClO_3$)	
10% of Oxalic Acids ($C_2H_2O_4$)	
Ruthenium (III) Chloride ($RuCl_3$)	
Citric Acid (CA)	
Ethylene Glycol (EG)	
Sodium Chloride (NaCl)	Electrolyte
Tris Hydrochloride	EPS test: protein and polysaccharides
Triton X-100	
Bicinchoninic Acid (BCA) Protein Assay Kit	
Sulfuric Acid	

Downloaded from http://iwaponline.com/wst/article-pdf/86/5/1122/1109750/wst086051122.pdf
by guest

2.3. Experimental procedures

Electrochemical oxidation was carried out in a 500-mL beaker with an electrode distance of 5 cm throughout the experiment in a fixed parallel manner with an effective electrode area of ~55 cm^2, to achieve high solubility of sludge (Ye *et al.* 2016). A constant speed of 300 rpm was applied throughout the experiment to ensure that the process was maintained at a homogeneous manner and to prevent any settlement of the sludge. The electrolyte used in this study was NaCl, where it has a trait in generating oxidant species that had the quality of showing higher reaction rates with organic compounds (Fajardo *et al.* 2017).

As the abovementioned, RSM type CCD was applied in order to identify the optimized operating conditions of the pre-treatment as a means to enhance sludge disintegration and dewaterability. CCD is known for its capability to analyze the relationship between independent factors and dependent responses. A five level factorial ($-\alpha$, −1, 0, +1, $+\alpha$) was applied in this analysis. Three independent variables were set: current density (A), electrolyte concentration (B) and electrolysis time (C). MLVSS removal, CST increment, EPS increment and sCOD increment were the responses of the pre-treatment as abovementioned. The range of each independent variables was inserted into Design Expert Software (version 11.1.2.0) to generate a set of 20 experimental runs that contained combinations of factorial runs, axial runs and center points. The number of runs was calculated using the equation (Equation (5)),

$$N = 2^n + 2n + n_c \tag{5}$$

whereby N = number of runs, n = number of factors and n_c = number for center points. Calculations of axial points can be obtained through a series of equations whereby these steps were easily calculated through the software. The complete ranges and level of independent variables are shown in Table 3. Analysis of variance (ANOVA) was used by the software to calculate the results (Isam *et al.* 2019).

2.4. Analytical methods

Standard method 2540E was applied for the measurement of MLVSS and its reduction was calculated. Standard method 5220D was used for the measurement of sCOD level after pre-treatment (APHA 2005). Furthermore, a CST apparatus (model: 304M Triton) was used to measure the dewaterability of the pre-treated sludge in seconds. Protein and polysaccharide are both common indicators for the quantification of EPS. The EPS increment was calculated by the increase in the summation of both protein and polysaccharide. The BCA method and the sulfuric-UV method were used to identify the protein and polysaccharide, respectively. The detection methods for EPS and sCOD were through a UV-vis spectrophotometer (model: JASCO V-730) and were calculated with the equations generated from the calibration curve.

3. RESULTS AND DISCUSSION

3.1. Morphology of Ti/RuO_2 electrodes

Figure 1 shows the morphology of the ruthenium oxide-coated titanium electrodes (Ti/RuO_2) with a magnification of ×500 and ×5,000, respectively using FESEM. It can be seen in Figure 1(a), that there was a rather even coated and distributed surface, which represents that EO could be carried out smoothly due to the high levels of active sites. In Figure 1(b), there were some minor 'cracked mud' surfaces detected. The contrast of the rate of expansion between the metal oxide film and the titanium substrate was the cause of the crack (Bezerra *et al.* 2020). This is a common phenomenon when coating with DSA as it involves different temperatures of heating. This may be possibly caused by the high rate of the heating process (Gonzaga *et al.* 2020). From the FESEM morphology, a multilayer coating of RuO_2 and a minimum occurrence of crack, portrayed the

Table 3 | Independent variables and ranges for RSM type CCD

			Levels and ranges				
Independent variable	**Unit**	**Code**	**Minimum**	**−1**	**0**	**+1**	**Maximum**
Current Density	mA/cm^2	A	1.14	10.0	23.0	36.0	44.86
Electrolyte Concentration	g/L	B	1.23	6.0	13.0	20.0	24.77
Electrolysis Time	minutes	C	9.50	30.0	60.0	90.0	110.45

Downloaded from http://iwaponline.com/wst/article-pdf/86/5/1122/1109750/wst086051122.pdf
by guest

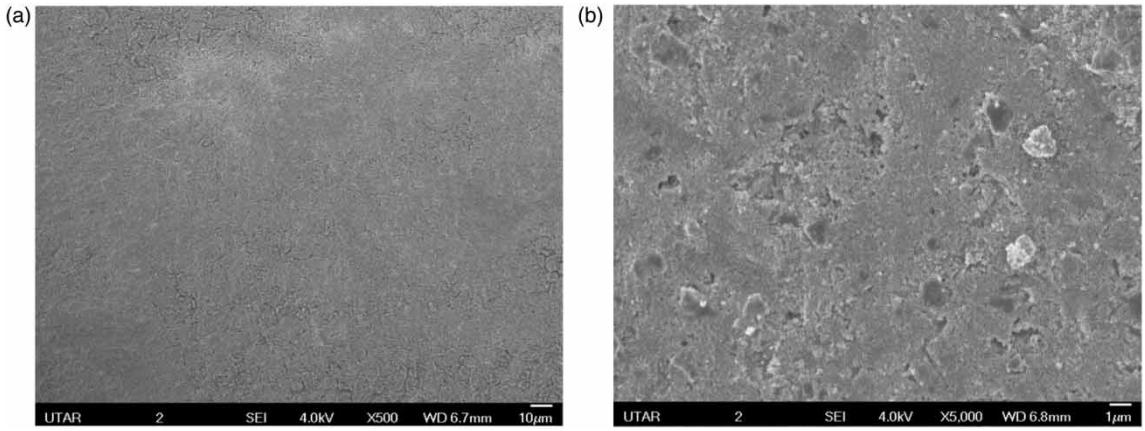

Figure 1 | FESEM image of Ti/RuO_2 at two magnifications (a) ×500 and (b) ×5,000.

stability of DSA as the electrolyte would be compromised when attacking the catalyst layer (Ajab *et al.* 2020). Moreover, from the outcome of EDX has shown an escalating percentage content of ruthenium which proves the coating's chemical composition (Bezerra *et al.* 2020). Another proof of even distribution and homogeneous coating can be seen from the energy dispersive spectroscopy (EDS) elemental mapping, as shown in Figure 2(a). In Figure 2(b), the elemental analysis revealed that the titanium electrode contained Ru (51.49% wt.), O (47.81% wt.) and Ti (0.70% wt.), indicating its high purity and suitability as a working electrode. The EDX result was consistent with the FESEM images, which clearly indicated that RuO_2 composite had been successfully deposited on the surface of the titanium plate.

3.2. RSM type CCD optimization

In this study, RSM type CCD was applied for optimization that generated 20 runs (14 non-center points and six center points), the experimental design data together with its responses are listed in Table 4.

The connection with the predictor variable and response variable were analyzed through the ANOVA. Four (4) regression polynomial equations (Equations (6)–(9)) were generated based on the four dependent variables with the indications of current density (A), electrolyte concentration (B) and electrolysis time (C) as the three independent variables. Based on the regression equations, there was an immediate positive effect between both the independent factors and the performance of dependent variables whereby the increase in the independent variable was able to improve the performance and vice versa (Moteshaker *et al.* 2020). Through the comparison of the coefficients among the regression equations in linear term, it helps to identify the relative impact of the variables (Hu *et al.* 2021). In this study, the coefficient of current density (A) had achieved the highest value among the predictor variables in terms of MLVSS removal, CST reduction and sCOD

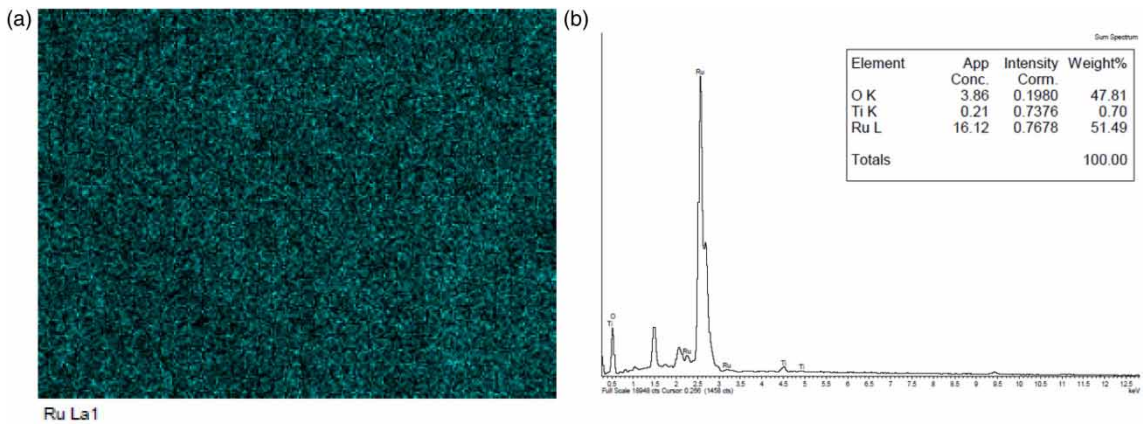

Figure 2 | (a) Elemental mapping with EDS analysis of coating and (b) elemental spectrum.

Downloaded from http://iwaponline.com/wst/article-pdf/86/5/1122/1109750/wst086051122.pdf
by guest

Table 4 | Experimental design and responses for the EO pre-treatment of POME WAS

	A: Current density (mA/cm^2)	B: Electrolyte concentration (g/L)	C: Electrolysis time (minutes)	MLVSS removal (%)	CST reduction (%)	EPS increment (%)	sCOD increment (%)
1	23	13	60	20.8	46.0	25.4	21.2
2	23	13	60	14.4	43.8	13.7	37.2
3	36	6	90	70.5	85.9	46.7	−10.2
4	10	6	90	21.5	27.5	38.2	45.7
5	23	24.77	60	24.6	40.0	30.4	39.4
6	23	13	9.5	5.6	21.3	93.4	46.5
7	1.14	13	60	7.0	8.5	10.4	18.1
8	23	13	60	19.8	40.6	12.4	24.1
9	23	13	60	20.7	45.7	18.4	35.0
10	36	6	30	20.5	22.6	64.3	25.8
11	10	6	30	19.0	11.5	43.8	64.7
12	23	13	110.5	57.0	78.3	61.2	5.2
13	23	1.23	60	30.2	38.8	7.1	25.1
14	44.86	13	60	63.1	84.9	25.9	−30.8
15	36	20	30	16.1	23.7	80.1	36.5
16	23	13	60	17.4	54.7	21.8	33.4
17	23	13	60	22.0	47.2	11.8	25.7
18	36	20	90	66.1	84.9	50.3	−18.9
19	10	20	90	7.4	19.9	48.0	15.6
20	10	20	30	19.4	12.6	65.9	33.7

increment of 14.66, 20.07 and 15.28, respectively. Hence, the equations showed that current density outperformed the electrolysis time and electrolyte concentration in terms of significance level. The coefficient of the variable signified its significance level in the further optimization study:

$$\text{MLVSS Removal} = 19.25 + 14.66A - 2.33B + 12.96C + 0.6162AB + 13.70AC - 1.82BC + 5.20A^2 + 2.49B^2 + 3.88C^2 \quad (6)$$

$$\text{CST Reduction} = 46.63 + 20.07A - 0.3201B + 17.83C + 0.8313AB + 12.65AC - 1.37BC - 1.81A^2 - 4.39B^2 - 0.7042C^2 \quad (7)$$

$$\text{EPS Increment} = 16.75 + 5.24A + 6.62B - 9.14C - 1.57AB - 2.99AC - 3.06BC + 3.56A^2 + 3.77B^2 + 24.45C^2 \quad (8)$$

$$\text{sCOD Increment} = 29.19 - 15.28A - 2.56B - 14.49C + 7.88AB - 6.78AC - 2.31BC - 11.05A^2 + 2.60B^2 + 0.3295C^2 \quad (9)$$

The ANOVA outputs were tabulated in Table 5. Coefficient of determination (R^2), level of significant (p-value) and the lack of fit test are the most representative indicators in proving the model's significance (Isam *et al.* 2019). R^2 and Adjusted R^2 (R^2_{adj}) were given more attention whereby R^2 is the extent of the level of response variability reduced through the independent variable of the model. R^2 reaching 1 is the most desirable value, to have a balanced match between experimental and predicted data. However, a minimum of 0.8 is sufficient (Darvishmotevalli *et al.* 2019). All of the dependent variables were able to achieve the minimum suggested value of R^2 i.e. $R^2_{MLVSS} = 0.9773$, $R^2_{CST} = 0.9610$, $R^2_{EPS} = 0.9230$ and

Downloaded from http://iwaponline.com/wst/article-pdf/86/5/1122/1109750/wst086051122.pdf
by guest

Table 5 | RSM type CCD ANOVA output table for four dependent variables

Source	Sum of squares	Degree of freedom	Mean square	F-value	*p*-value	Remarks
MLVSS Removal						
Model	7,228.77	9	825.42	47.74	<0.0001	Significant
Residual	172.90	10	17.29	–	–	–
Lack of Fit	134.00	5	26.80	3.44	0.1004	Not significant
$\mathbf{R^2 = 0.9773\ R^2_{adj} = 0.9568\ R^2_{pred} = 0.85347\ AP = 22.8731}$						
CST Reduction						
Model	1,451.71	9	27.39	27.39	<0.0001	Significant
Residual	464.57	10	46.46	–	–	–
Lack of Fit	353.93	5	70.79	3.20	0.1138	Not significant
$\mathbf{R^2 = 0.9610\ R^2_{adj} = 0.9259\ R^2_{pred} = 0.7614\ AP = 17.2987}$						
EPS Increment						
Model	10,953.85	9	1,217.08	13.32	0.0002	Significant
Residual	913.92	10	91.39	–	–	–
Lack of Fit	760.54	5	152.11	4.94	0.0521	Not significant
$\mathbf{R^2 = 0.9230\ R^2_{adj} = 0.8537\ R^2_{pred} = 0.4979\ AP = 12.5927}$						
sCOD Increment						
Model	9,032.58	9	1,003.62	10.51	0.0005	Significant
Residual	954.92	10	95.49	–	–	–
Lack of Fit	737.71	5	147.54	3.40	0.1029	Not significant
$\mathbf{R^2 = 0.9044\ R^2_{adj} = 0.8183\ R^2_{pred} = 0.4003\ AP = 11.9074}$						

$R^2_{sCOD} = 0.9044$. On top of that, the closeness between R^2 and R^2_{adj}, i.e. $R^2_{adj\ MLVSS} = 0.9568$, $R^2_{adj\ CST} = 0.9259$, $R^2_{adj\ EPS} = 0.8537$ and $R^2_{adj\ sCOD} = 0.8183$ indicated that there were no chances of insignificance within the model (Ken & Sinha 2021).

Moreover, a *p*-value <0.05 should be assured as it serves as evidence that the model is significant (Darvishmotevalli *et al.* 2019). The RSM type CCD ANOVA output tables for the four variables (linear, two-way interactions and quadratic) are attached in Tables S1–S4 as supplementary material. From the table, all variables were able to achieve a relatively low *p*-value where the *p*-values for MLVSS and CST were <0.0001, whereas the *p*-values for EPS and sCOD were 0.0002 and 0.0005, respectively. Furthermore, a lack of fit of test should be 'not significant' as it proves that the model is able to be fitted. All four dependent variables were able to achieve, however, a probability lack of fit (PLOF) of EPS that showed a lower percentage among the other three variables. This portrays that there was a lower chance that EPS will not be fitted due to noise. Lastly, the measurement of the ratio between signal to noise is termed as the adequate precision (AP) (Moteshaker *et al.* 2020). It shows the comparison between the ranges of values predicted at design points with the mean prediction error. All of the AP exceeded the minimum value of 4, means that the maneuvering of design space could take place through the models (Isam *et al.* 2019).

3.3. Three-dimensional surface plot and process optimization by RSM type CCD

The three-dimensional surface plots of each response variables are shown in Figure 3 with current density (mA/cm^2) and electrolysis time (minutes) as the axis due to their higher significance level, as discussed in the previous section.

3.3.1. Effect of current density

From the surface plots (Figure 3(a)–3(c)), MLVSS removal, CST reduction and EPS increment were shown to be increasing as the current density increased. This can be explained due to the ion species that were formed that possessed the robust affinity to treat the organic matter within the WAS. Higher current promotes more electrons flowing and thus enhancies the rate of oxidation. High resistance within the reaction is not the only factor to be affected. To further explain this, secondary oxidizing

Downloaded from http://iwaponline.com/wst/article-pdf/86/5/1122/1109750/wst086051122.pdf
by guest

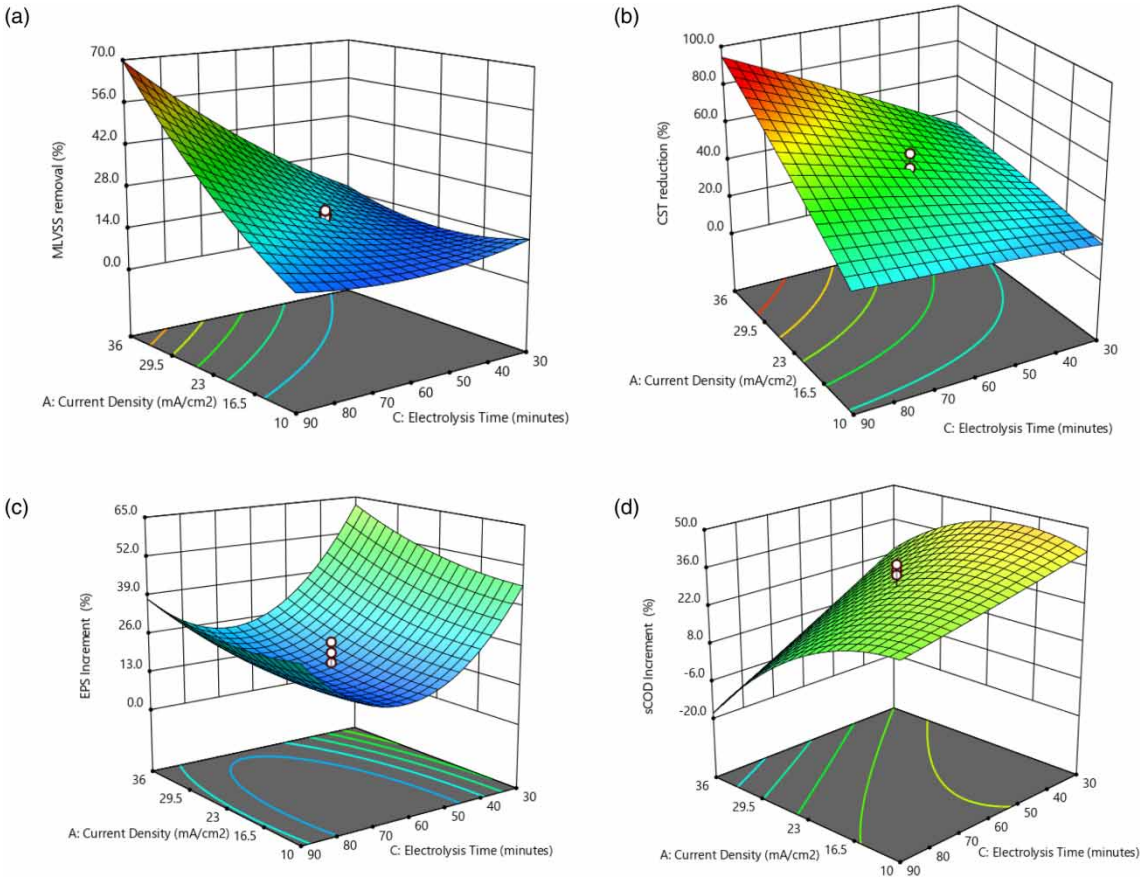

Figure 3 | Three-dimensional response surface plots of (a) MLVSS removal; (b) CST reduction; (c) EPS increment and (d) sCOD increment between current density and electrolysis time at 13 g/L of NaCl concentration.

agents will be created due to the oxidation of organic matter. These secondary oxidizing agents tend to be weaker and are unable to perform as well as •OH radicals, which will cause mineralization to take place and influence the post-treatment (Pérez-Rodríguez *et al.* 2019). As mentioned, pre-treatment efficiency is dependent on the amount of oxidizing agents being created, the increase in current density only affects direct oxidation as strong oxidizing agents are formed at the surface of the electrodes. Although, the higher the current density the better the efficiency, particularly in removing the WAS solid content. However, the amount of voltage being applied needs to be taken into consideration as it would be less economical or possibly side reactions might occur that would deteriorate the overall performance, especially on the sCOD solubilization beyond ~23 mA/cm^2, as shown in Figure 3(d). This is in close agreement with Pasalari and his co-researchers who found that no biodegradability would be promoted in terms of sCOD in the EO process when the current density reached 30–40 mA/cm^2 (Pasalari *et al.* 2021). It is important to understand that the restriction of current density is necessary as voltage increases, heat would be dissipated leading to other side effects (Hu *et al.* 2021). Not only that, the operating conditions of the EO pre-treatment should be applied to help in solubilizing the organic matter in order to enhance biodegradability and overcome the hydrolysis problem in AD. High current density would lead to the mineralization of organic molecules instead of solubilizing them (Barrios *et al.* 2021).

3.3.2. Effect of electrolysis time

Electrolysis time is considered as one of the few vital parameters that would affect the performance of EO. From the surface plots, MLVSS removal and CST reduction were directly proportional towards the electrolysis time, as shown in Figure 3(a) and 3(b), due to the increased level of oxidizing agents (•OH radicals). The electrolysis time had more effect with higher current density, in terms of MLVSS removal. Both of the independent variables had inseparable relationship whereby a balance

Downloaded from http://iwaponline.com/wst/article-pdf/86/5/1122/1109750/wst086051122.pdf
by guest

needed to be achieved when the voltage of the system was higher, and a lower electrolysis time is needed to achieve a certain level of solubilization (Rodriguez *et al.* 2018). However, there would be decay in organic matter if the duration is too long. The sCOD increment was enhanced by electrolysis time at the beginning of the EO and dropped further after the peak at 30 min, as shown in Figure 3(d). According to Pasalari *et al.* (2021), sCOD concentration would increase sharply at the beginning of the pre-treatment, which showed that intracellular materials were released into the aqueous phase, thus enhancing the biodegradability of the WAS. This was due to the electromigration of ions at the beginning of the EO. Inorganic matter is released into the liquid phase through solubilization. The accumulation of ions or organic matters takes place at both electrodes and hence causes a blockage that increases the current resistance and restricts the process's ability to take place correctly (Heidari *et al.* 2020). Due to the increase in current resistance, the current drops gradually throughout the entire process, which affected the performance of the sCOD increment. The decrease in concentration of sCOD most likely occurred at extremely high current density at 44.86 mA/cm^2 or due to the high electrolysis time at 90 min from the results. This could be explained by the rapid sCOD mineralization of dissolved organic substances compared with solubilization.

3.3.3. Effect of electrolyte (NaCl) concentration

Electrolyte (NaCl) concentration was fixed at the middle level set due to its least significant level. NaCl helps in preventing the formation of oxidizing layers by other anions and causes ohmic resistance within the cell and thus prevents the decline in COD removal. However, depletion in sCOD due to mineralization is not desired as it would further affect the biogas generation in the subsequent AD. From the results, a slight drop in sCOD occurred as the NaCl concentration increased, as well as the EPS concentrations. This could be due to the presence of negative charges at the bacteria surfaces that generate a high electrostatic repulsive force that leads to the occurrence of sludge disintegration (Heng *et al.* 2021). MLVSS removal and CST reduction rate showed no effect on the increase in NaCl concentration.

3.4. Validation of the model

The applicability of the mathematical model can be assessed by diagnostic plots, to show the predicted versus observed values of percentage of each dependent variables (Figure 4). The predicted and experimental values are close to a straight line. This trend indicated that the predicted values using the calibrated models were highly correlated with the actual values of MLVSS removal, CST reduction, EPS increment and sCOD increment. It also indicated a close agreement between experimental results and predicted values, with a high R^2 of 0.9044–0.9773. Therefore, the models can be used to predict the studied responses, which confirmed the good predictive quality of the models.

3.5. Optimization

The optimization process was done by inserting the minimum or maximum desired values for the response variables. In order to have a better WAS disintegration and dewaterability, minimum MLVSS removal, CST reduction and sCOD increment but maximum EPS increment were set. All three factors were taken into considerations with different weightage, the criteria were set at MLVSS removal >20%, CST reduction >43%, EPS increment <19% and sCOD increment >25%. An overlay plot shown in Figure 5 was generated, which was based on a specific criterion portraying a visual selection of ideal conditions. The shaded region showed that the criteria could be met when the range for the optimum operating conditions was followed, i.e. current density (17–27 mA/cm^2) and electrolysis time (55–75 minutes) at a fixed concentration of NaCl (10 g/L). The observed results were similar to those reported in the literature (Barrios *et al.* 2021; Pasalari *et al.* 2021), which recommended electrolysis working at a current density lower than 30 mA/cm^2, to prevent the acceleration of organic matter mineralization from happening. Thus, it is advisable to limit the current density to avoid adverse effects such as heat generation and higher power consumption.

Pre-treatments were performed aiming to enhance the digestibility of WAS, which in turn improved the performance of AD. The best way to indicate AD performance was through biogas yield and different studies have been carried out showing that pre-treatment was able to improve biogas yield. Huang *et al.* (2021) showed that an sCOD increment from 29 to 350 mg/L successfully increased the methane yield (from 105 to 134 mL CH_4/g VSS) using an electrochemical pre-treatment (Ti/RuO_2) on municipal WAS. Another study proved that biogas generation from 109 N-L CH_4/kg.VS in non-pretreated WAS increased to 311.9 $\pm$ 6 N-L CH_4/kg.VS using electrochemical pre-treatment at a current density of 28.6 mA/cm^2 (Barrios *et al.* 2021).

Downloaded from http://iwaponline.com/wst/article-pdf/86/5/1122/1109750/wst086051122.pdf
by guest

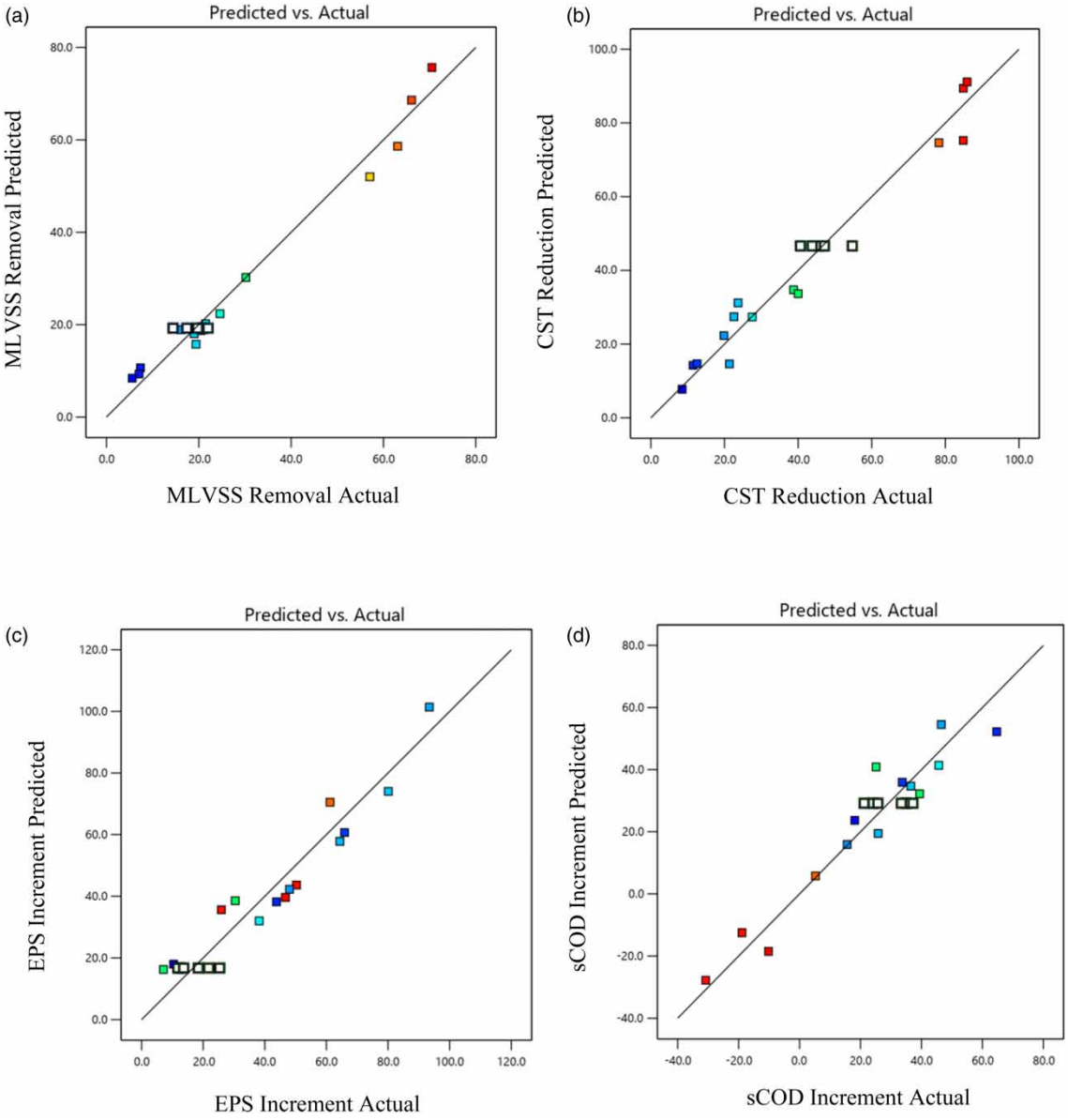

Figure 4 | Correlation between predicted and actual values for (a) MLVSS removal, (b) CST reduction, (c) EPS increment and (d) sCOD increment.

4. CONCLUSIONS

The generation of POME WAS has gradually increased over many years due to the development of the palm oil industry. It is important that the generated sludge is treated before being released into the environment. The EO process using Ti/RuO_2 was used in this study. FESEM surface images and EDS elemental analysis of the Ti/RuO_2 electrodes indicated that the preparation following Pechini's method can produce a uniform and homogeneous coating throughout the titanium plate. An RSM type CCD was successfully applied to describe the EO process using a second-order model. The most significant effects on WAS disintegration and dewaterability were found to be due to current density and electrolysis time, while the influence of NaCl concentration was relatively insignificant. The model exhibited that the suggested model agreed well with experimental results with high R^2 values (0.9044–0.9773) for all the studied dependent variables. The optimum operating conditions were in the range of current density 17–27 mA/cm^2 and electrolysis time 55–75 minutes, at a fixed

Downloaded from http://iwaponline.com/wst/article-pdf/86/5/1122/1109750/wst086051122.pdf
by guest

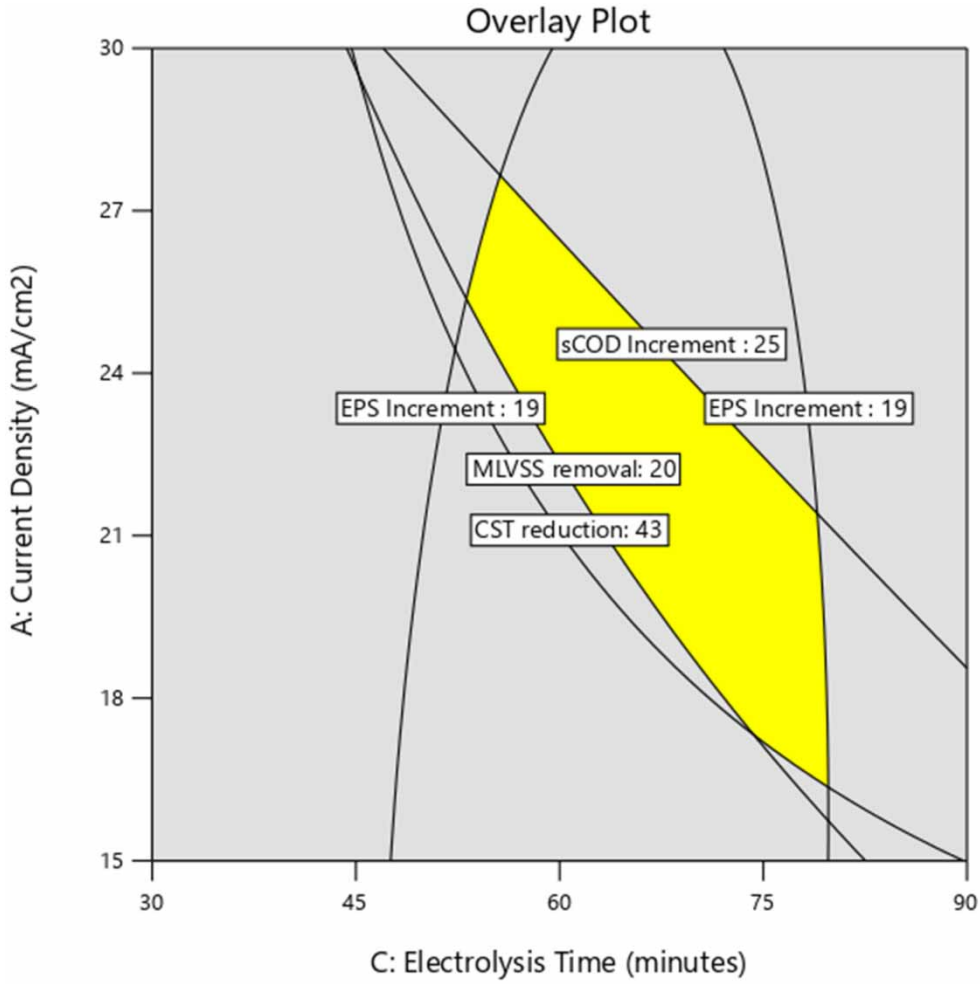

Figure 5 | Overlay plot for optimal region at electrolyte concentration 10 g/L.

concentration of NaCl (10 g/L), resulting in MLVSS removal >20%, CST reduction >43%, EPS increment <19% and sCOD increment >25%. Consequently, these results proved that Ti/RuO_2 could play an important role in the pre-treatment of POME WAS in sludge disintegration and adequate dewaterability, for the subsequent AD to further enhance the solid removal and biogas generation.

ACKNOWLEDGEMENTS

The authors are thankful to Universiti Tunku Abdul Rahman (UTAR), Malaysia for providing facilities and support for this research. This work was funded by the UTAR Research Fund under project number IPSR/RMC/UTARRF/2019-C1/G01.

DATA AVAILABILITY STATEMENT

All relevant data are included in the paper or its Supplementary Information.

CONFLICT OF INTEREST

The authors declare there is no conflict.

REFERENCES

Ajab, H., Isa, M. H. & Yaqub, A. 2020 Electrochemical oxidation using Ti/RuO_2 anode for COD and PAHs removal from aqueous solution. *Sustain. Mater. Technol.* **26**, e00225. doi:10.1016/j.susmat.2020.e00225.

Downloaded from http://iwaponline.com/wst/article-pdf/86/5/1122/1109750/wst086051122.pdf
by guest

APHA 2005 *Standard Methods for the Examination of Water and Wastewater*, 21st edn. American Public Health Association/American Water Works Association/Water Environment Federation, Washington DC, USA.

Barrios, J. A., Cano, A., Rivera, F. F., Cisneros, M. E. & Duran, U. 2021 Efficiency of integrated electrooxidation and anaerobic digestion of waste activated sludge. *Biotechnol. Biofuels* **14** (1), 81. doi:10.1186/s13068-021-01929-7.

Bezerra, C. W. A., Santos, G. O. S., Pupo, M. M. S., Gomes, M. A., Silva, R. S., Eguiluz, K. I. B. & Salazar-Banda, G. R. 2020 Novel eco-friendly method to prepare Ti/RuO_2–IrO_2 anodes by using polyvinyl alcohol as the solvent. *J. Electroanal. Chem.* **859**, 113822. doi:10.1016/j.jelechem.2020.113822.

Darvishmotevalli, M., Zarei, A., Moradnia, M., Noorisepehr, M. & Mohammadi, H. 2019 Optimization of saline wastewater treatment using electrochemical oxidation process: prediction by RSM method. *MethodsX* **6**, 1101–1113. doi:10.1016/j.mex.2019.03.015.

Fajardo, A. S., Seca, H. F., Martins, R. C., Corceiro, V. N., Freitas, I. F., Quinta-Ferreira, M. E. & Quinta-Ferreira, R. M. 2017 Electrochemical oxidation of phenolic wastewaters using a batch-stirred reactor with NaCl electrolyte and Ti/RuO_2 anodes. *J. Electroanal. Chem.* **785**, 180–189. doi:10.1016/j.jelechem.2016.12.033.

Gonzaga, I. M. D., Dória, A. R., Vasconcelos, V. M., Souza, F. M., Santos, M. C., Hammer, P., Rodrigo, M. A., Eguiluz, K. I. B. & Salazar-Banda, G. R. 2020 Microwave synthesis of Ti/$(RuO_2)_{0.5}(IrO_2)_{0.5}$ anodes: improved electrochemical properties and stability. *J. Electroanal. Chem.* **874**, 114460. doi:10.1016/j.jelechem.2020.114460.

Heidari, M., Vosoughi, M., Sadeghi, H., Dargahi, A. & Mokhtari, S. A. 2020 Degradation of diazinon from aqueous solutions by electro-Fenton process: effect of operating parameters, intermediate identification, degradation pathway, and optimization using response surface methodology (RSM). *Sep. Sci. Technol.* **56** (13), 2287–2299. doi:10.1080/01496395.2020.1821060.

Heng, G. C., Isa, M. H., Lock, S. S. M. & Ng, C. A. 2021 Process optimization of waste activated sludge in anaerobic digestion and biogas production by electrochemical pre-treatment using ruthenium oxide coated titanium electrodes. *Sustainability* **13** (9), 4874. doi:10.3390/su13094874.

Hu, X., Dong, H., Zhang, Y., Fang, B. & Jiang, W. 2021 Mechanism of *N,N*-dimethylformamide electrochemical oxidation using a Ti/RuO_2 – IrO_2 electrode. *RSC Adv.* **11** (13), 7205–7213. doi:10.1039/D0RA10181H.

Huang, H., Zeng, Q., Heynderickx, P. M., Chen, G.-H. & Wu, D. 2021 Electrochemical pretreatment (EPT) of waste activated sludge: extracellular polymeric substances matrix destruction, sludge solubilisation and overall digestibility. *Bioresour. Technol.* **330**, 125000. doi:10.1016/j.biortech.2021.125000.

Isam, M., Baloo, L., Kutty, S. R. M. & Yavari, S. 2019 Optimisation and modelling of Pb(II) and Cu(II) biosorption onto red algae (*Gracilaria changii*) by using response surface methodology. *Water* **11** (11), 2325. doi:10.3390/w11112325.

Iskurt, C., Keyikoglu, R., Kobya, M. & Khataee, A. 2021 Treatment of coking wastewater by aeration assisted electrochemical oxidation process at controlled and uncontrolled initial pH condition. *Sep. Purif. Technol.* **248**, 117043. doi:10.1016/j.sep.pur.2020.117043.

Jiang, Y., Zhao, H., Liang, J., Yue, L., Li, T., Luo, Y., Liu, Q., Lu, S., Asiri, A. M., Gong, Z. & Sun, X. 2021 Anodic oxidation for the degradation of organic pollutants: anode materials, operating conditions and mechanisms. A mini review. *Electrochem. Commun.* **123**, 106912. doi:10.1016/j.elecom.2020.106912.

Johnson, I. & Kumar, M. 2020 Electrochemical oxidation of distillery wastewater by dimensionally stable Ti-RuO_2 anodes. *Environ. Technol. Inno.* **20**, 101181. doi:10.1016/j.eti.2020.101181.

Kamyab, H., Chelliapan, S., Din, M., Rezania, S., Khademi, T. & Kumar, A. J., 2018 Palm Oil Mill Effluent as an Environmental Pollutant. In: *Palm Oil* (Waisundara, V. ed.). IntechOpen. doi:10.5772/INTECHOPEN.75811.

Kang, J., Gwon, Y. R. & Cho, S. K. 2020 Photoelectrochemical water oxidation on $PbCrO_4$ thin film photoanode fabricated via Pechini method: various solution-processes for $PbCrO_4$ film synthesis. *J. Electroanal. Chem.* **878**, 114601. doi:10.1016/j.jelechem.2020.114601.

Ken, D. S. & Sinha, A. 2021 Dimensionally stable anode (Ti/RuO_2) mediated electro-oxidation and multi-response optimization study for remediation of coke-oven wastewater. *J. Environ. Chem. Eng.* **9** (1), 105025. doi:10.1016/j.jece.2021.105025.

Moteshaker, P. M., Rokni, S. E., Farnoodian, N., Akhlaghi, N. M., Saadi, S., Ahmadidoust, G. & Yousefi, A. 2020 Application of response surface methodology for optimization of electrochemical process in metronidazole (MNZ) removal from aqueous solutions using stainless steel 316 (SS316) and lead (Pb) anodes. *Int. J. Chem. React. Eng.* **18** (8), 20200055. doi:10.1515/ijcre-2020-0055.

Nurhayati, E., Bagastyo, A. Y. & Hartatik, D. D. 2020 Effect of flow rate on electrochemical oxidation of landfill leachate using DSA and BDD anode. *IOP Conf. Ser. Earth Environ. Sci.* **506**, 012038.

Pasalari, H., Esrafili, A., Rezaee, A., Gholami, M. & Farzadkia, M. 2021 Electrochemical oxidation pretreatment for enhanced methane potential from landfill leachate in anaerobic co-digestion process: Performance, Gompertz model, and energy assessment. *Chem. Eng. J.* **422**, 130046. doi:10.1016/j.cej.2021.130046.

Pérez-Rodríguez, M., Cano, A., Durán, U. & Barrios, J. A. 2019 Solubilization of organic matter by electrochemical treatment of sludge: influence of operating conditions. *J. Environ. Manage.* **236**, 317–322. doi:10.1016/j.jenvman.2019.01.105.

Rodriguez, F. A., Pivero, E. P. & Gonzalez, I. 2018 Adapted Pechini method to prepare DSA type electrodes of RuO_2-ZrO_2 doped with Sb_2O_5 over titanium plates. *MethodsX* **5**, 1613–1617. doi:10.1016/j.mex.2018.11.020.

Ye, C., Yuan, H., Lou, Z. & Zhu, N. 2016 Combined electrochemical and hypochlorite pretreatment for improving solubilization and anaerobic digestion of waste-activated sludge: effect of hypochlorite dosage. *Energy Fuels* **30** (4), 2990–2996. doi:10.1021/acs.energyfuels.5b02884.

Zhu, X., Hu, W., Feng, C., Chen, H., Chen, N. & Li, R. 2019 Electrochemical oxidation of aniline in sodium chloride solution using Ti/RuO_2 anode. *Int. J. Electrochem. Sci.* **14**, 7516–7528. doi:10.20964/2019.08.36.

First received 17 June 2022; accepted in revised form 5 August 2022. Available online 16 August 2022

Downloaded from http://iwaponline.com/wst/article-pdf/86/5/1122/1109750/wst086051122.pdf
by guest